

Associations of Hurricane Intensity Changes to Satellite Total Column Ozone Structural Changes Within Hurricanes

Lin Lin[✉] and Xiaolei Zou[✉], *Member, IEEE*

Abstract—Hurricane top structures are not well captured by airborne or dropsonde observations. Total column ozone (TCO) observations provided by the Ozone Mapping and Profiler Suite (OMPS) Nadir Mapper (NM) onboard the Suomi National Polar-orbiting Partnership (S-NPP) satellite are employed in an investigation of hurricane top structures. We show that the OMPS NM TCO data can capture the top structures of Hurricane Maria (2017) over the Atlantic Ocean. An observed local maximum of TCO in the eye region reveals a strong upper tropospheric downward motion that lowers the tropopause above the hurricane eye. A rainband-like distribution of low TCO content reflects strong convection areas where the tropopause is raised and well correlates spatially with the high cloud top regions derived from the S-NPP Visible Infrared Imaging Radiometer Suite (VIIRS). A sixth-order even polynomial fitting is used to reveal the TCO radial structures by introducing two characteristic parameters. One is a radial distance parameter (R_{TCO}) representing the spatial range, and the other is an intensity parameter defined as the TCO difference from the hurricane center to 600-km radial distance from the hurricane center ($\Delta\text{TCO}_{600\text{km}}$). Based on an analysis of ten hurricanes over the Northern Atlantic Ocean in 2017, we show that before a hurricane reaches its maximum strength, there is always a decrease of R_{TCO} and an increase of $\Delta\text{TCO}_{600\text{km}}$. It is anticipated that more accurate initial hurricanes could be produced if the TCO structures were combined with other surface, near surface, and tropospheric information in vortex initialization.

Index Terms—Hurricane intensity change, ozone from Suomi National Polar-orbiting Partnership (S-NPP) Ozone Mapping and Profiler Suite (OMPS), remote sensing.

I. INTRODUCTION

THE stratosphere is an ozone-rich layer. The total ozone in a column of the atmosphere (called the total column ozone, TCO, hereafter for brevity) is directly related to the

Manuscript received March 9, 2021; revised May 16, 2021; accepted June 20, 2021. Date of publication July 15, 2021; date of current version January 14, 2022. The work of Xiaolei Zou was supported by the National Key Research and Development Program of China under Grant 2018YFC1507004. The work of Lin Lin was supported by the U.S. Department of Commerce under National Oceanic and Atmospheric Administration (NOAA) Grant “NA19NES4320003” (Cooperative Institute for Satellite Earth System Studies—CISESS) at the Earth System Science Interdisciplinary Center (ESSIC), University of Maryland. (*Corresponding author: Xiaolei Zou.*)

Lin Lin is with the Earth System Science Interdisciplinary Center (ESSIC), University of Maryland, College Park, MD 20740 USA (e-mail: linlin@umd.edu).

Xiaolei Zou is with the Joint Center of Data Assimilation for Research and Application, Nanjing University of Information and Science and Technology, Nanjing, Jiangsu 210044, China (e-mail: xzou@nuist.edu.cn).

Digital Object Identifier 10.1109/TGRS.2021.3094107

stratospheric depth. Temporal and spatial variations in TCO at large scales are mainly caused by large-scale advection and vertical motion, while small-scale variations in TCO are associated with smaller-scale convection in the atmosphere [1]. The stratosphere is also a high potential vorticity (PV) layer. Therefore, in middle and high latitudes, regions with high TCO amounts are often associated with high column-integrated mean PV [2], [3]. Due to the close correlation between TCO and PV, variations in TCO in space and time could be used for studying PV-sensitive meteorological phenomena. For example, storm tracks based on the fluctuations of TCO observations from the total ozone mapping spectrometer (TOMS) were identified [4]. Davis *et al.* [5] retrieved 3-D winds directly from global TOMS TCO fields. The proximity between TCO and column-integrated mean PV on synoptic scales inspired scientists to use TCO data for improving mid-latitude cyclone predictions through data assimilation [6], [7]. A linear regression model that maps the column-integrated mean PV into the TCO field was used as an observation operator for TOMS TCO data assimilation, which improved the prediction of the track, intensity, and quantitative precipitation forecast skill of the mid-latitude winter storm that occurred on January 24–25, 2000, along the east coast of the US.

In the tropical and subtropical regions, the correlation between ozone and the column-integrated mean PV is generally much weaker than that at middle and high latitudes. By dividing the TCO field in a model domain into two different regimes, namely, one with strong and the other with weak deep convection/southerly advection, a linear regression model that links TOMS TCO observations to a model’s column-integrated mean PV fields can be developed for low latitudes by using only those TOMS TCO data in hurricane environments with weak convection [8]. Wu and Zou [7], subsequently, used this model for TOMS TCO data assimilation and showed a consistent improvement in the hurricane track prediction of Hurricane Erin (2001) due to a better forecast of the steering flow.

In regions of strong convection that push the tropopause upward, TCOs are generally low. TOMS TCO observations have revealed many interesting structural features of hurricanes that are large in horizontal scales, deep in vertical extents, and heterogeneous with strong vertical motions. The strong upward motion associated with strong convection results in rainband-like TCO lows within hurricanes. An upper-level downward

motion in the hurricane eye producing a local maximum in the TCO field near the hurricane center that is embedded in the TCO low was found using TOMS raw TCO data [8]. The existence of local ozone maxima in tropical cyclone (TC) centers seen from flight observations was reported earlier [9].

This study is an extension of Zou and Wu [8] that uses TCO observations from the Ozone Mapping and Profiler Suite (OMPS) Nadir Mapper (NM) onboard NOAA's Polar Operational Environmental Satellite—Suomi National Polar-orbiting Partnership (S-NPP). An advantage of using OMPS TCO observations for hurricane studies is the availability of simultaneous day-night-band (DNB) radiance observations and cloud top pressure retrievals from the Visible Infrared Imaging Radiometer Suite (VIIRS) that is also onboard the S-NPP satellite. The rainband-like distributions of TCO lows can be verified by DNB observations and cloud top pressure retrievals. In addition, we show that there is a distinguishable linkage between the OMPS TCO structure and hurricane intensity change within a 600-km radial distance from the hurricane center. Usually, there is a drop of TCO in a small region close to the hurricane center before the hurricane reaches its maximum strength. This finding would lead to an innovative TC vortex initiation by adding the TC structural information in OMPS TCO observations.

This article is arranged as follows: Section II describes TCO observations from the S-NPP OMPS NM and hurricane cases used in this study. Structural features of OMPS TCO observations and VIIRS cloud top pressure for Hurricane Maria are illustrated in Section III. The methodology used to characterize the OMPS TCO structure near the hurricane center and the quality control used in this study are described in Section IV. The associations of hurricane intensity changes to OMPS TCO within hurricanes for nine Atlantic TCs in 2017 are discussed in Section V. Section VI provides a summary and conclusions.

II. DATA AND CASE DESCRIPTION

The OMPS NM is a cross-track instrument that provides 105 cross-track field-of-views within the scan angle range of $\pm 110^\circ$ [10], [11]. The OMPS NM data used in this study are from the medium-resolution mode ($17 \times 17 \text{ km}^2$ at nadir and $40 \times 40 \text{ km}^2$ at the edges). TCO data at a medium resolution better capture small-scale features, especially the local maximum of TCO in the hurricane eye than do low-resolution TCO observations. The latter has a data resolution of $50 \times 50 \text{ km}^2$ at nadir and $120 \times 120 \text{ km}^2$ at the edges.

The TCO product used here is generated from the NOAA Joint Polar Satellite System OMPS Version 8 Total Ozone (V8TOz) algorithm. The V8TOz algorithm is based on the backscattered ultraviolet (BUV) total ozone algorithm originally proposed by Dave and Mateer [12] to process Nimbus-4 BUV data [13]. Radiance measurements from 12 BUV wavelengths (308.7, 310.8, 311.9, 312.61, 313.2, 314.4, 317.6, 322.4, 331.3, 345.4, 360.2, and 372.8 nm) are used to determine the TCO amount by separating the effects of ozone absorption from clouds and ground reflection and scattering [14]. It has been shown that the TCO from the V8TOz algorithm has stable, small biases on the order of -3% when compared to other TCO records [15].

TABLE I
SUMMARY OF TEN HURRICANES OVER THE
NORTHERN ATLANTIC OCEAN IN 2017

Name	Category	First time reached the maximum strength	Period
FRANKLIN	H1	0000UTC 10 August	August 6–10
GERT	H2	0000UTC 17 August	August 13–17
HARVEY*	H4	0000UTC 26 August	August 17–31
IRMA	H5	0600UTC 6 September	August 30–September 12
JOSE	H4	0000UTC 9 September	September 5–22
KATIA	H2	1800UTC 8 September	September 5–9
LEE	H3	1800UTC 27 September	September 15–30
MARIA	H5	0000UTC 20 September	September 16–30
NATE	H1	1800UTC 7 October	October 4–8
OPHELIA	H3	1200UTC 14 October	October 9–16

*: hurricane excluded due to the SLP_{\min} occurred near the coastline.

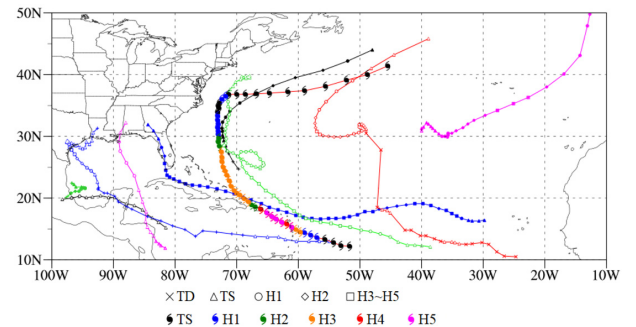


Fig. 1. Best tracks of Hurricanes Franklin (black open symbol), Gert (black solid symbol), Harvey (blue open symbol), Irma (blue solid symbol), Jose (green open symbol), Katia (green solid symbol), Lee (red open symbol), Nate (purple open symbol), and Ophelia (purple solid symbol) in 2017 at 6-h intervals. The following symbols are used for TD (cross), TS (open triangle), H1 (open circle), H2 (open diamond), H3–H5 (open square) for Franklin, Harvey, Joe, Lee, and Nate in the “open symbol” set, and TD (plus), TS (solid triangle), H1 (solid circle), H2 (solid diamond), and H3–H5 (solid square) for Gert, Irma, Katia, Maria, and Ophelia in the “solid symbol” set. The track of Hurricane Maria from 0000 UTC September 17 to 1800 UTC September 30, 2017, at 6-h intervals is indicated by the hurricane symbols as shown in the color bar.

In this study, a TCO dataset for the Atlantic (ATL) TCs in 2017 is used. It includes ten named storms that reached category 1–5 hurricane stages based on the best track data from HURDAT2 (Table I) [16]. The best tracks of these ten ATL TCs are shown in Fig. 1. Because the OMPS NM has a bandwidth of 2800 km, it cannot observe all TCs. To be included in the TCO dataset of this study, an overpass must capture a 600-km radius from the TC center. Moreover, at the OMPS observation time, the storm must be over the ocean when it reaches its minimum sea level pressure (SLP). The cyan symbols in Fig. 2 represent the time when the TC reached the lowest SLP. Hurricane Harvey was excluded in the following analysis because its lowest SLP occurred close to the coastline (blue open symbol).

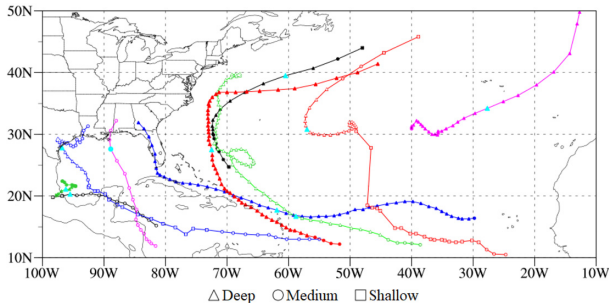


Fig. 2. Best tracks of Hurricanes Franklin (black open symbol), Gert (black solid symbol), Harvey (blue open symbol), Irma (blue solid symbol), Joe (green open symbol), Katia (green solid symbol), Lee (red open symbol), Maria (red solid symbol), Nate (purple open symbol), and Ophelia (purple solid symbol) in 2017 at 6-h intervals. The following symbols are used for deep (open triangle), medium (open circle), and shallow (open square) for Franklin, Harvey, Joe, Lee, and Nate in the “open symbol” set, and deep (solid triangle), medium (solid circle), and shallow (solid square) for Gert, Irma, Katia, Maria, and Ophelia in the “solid symbol” set. Cyan symbols indicate deep (solid cyan triangle), medium (solid cyan circle), and shallow (solid cyan square) at the time when the hurricane reaches its minimum SLP.

III. STRUCTURAL FEATURES OF HURRICANE MARIA FROM OMPS TCO AND VIIRS DATA

Among the nine selected ATL TCs, Hurricane Maria was the second category 5 hurricane to threaten the Leeward Islands two weeks after the passage of the first category 5 hurricane, i.e., Irma, during the hyperactive Atlantic hurricane season of 2017. Hurricane Maria experienced a rapid intensification from a tropical storm to a category 5 hurricane during September 17–19, 2017. It oscillated between categories 4 and 5 during September 19–20, 2017. It briefly weakened to a category 2 hurricane on September 21 and went back to category 3 status during September 21–24, 2017, as it moved over and away from the Leeward Islands. After this period, it started to weaken and experienced a sharp track change, moving from northward to eastward as it entered the mid-latitudes (the curve with hurricane symbols in Fig. 1).

The 3-D transport processes near the tropopause, and not tropospheric ozone, mostly contribute to the satellite-observed TCO distributions [17]. Fig. 3 presents the OMPS TCO on September 17, 19, and 23, 2017, respectively. The best track hurricane center location is indicated by the black hurricane symbol. VIIRS observations are available at the same time as OMPS TCO observations. Compared with VIIRS DNB radiance observations (figures omitted), spiral rainband features are only partially captured by OMPS TCO observations. Areas of low TCO are located in areas of convection, but areas of convection do not overlap with areas of low TCO. The transport processes associated with the convective upward motion in low clouds will have little impact on the transport of TCO in the stratosphere. Hence, we believe that S-NPP OMPS TCO observations mostly reflect the top structures of hurricanes.

Since the clouds reach different altitudes, an exact match in intensity between TCO and VIIRS DNB observations is not expected. On the other hand, the cloud top pressures retrieved by S-NPP OMPS TCO observations (Fig. 4) for Hurricane Maria at the same time as TCO observations shall

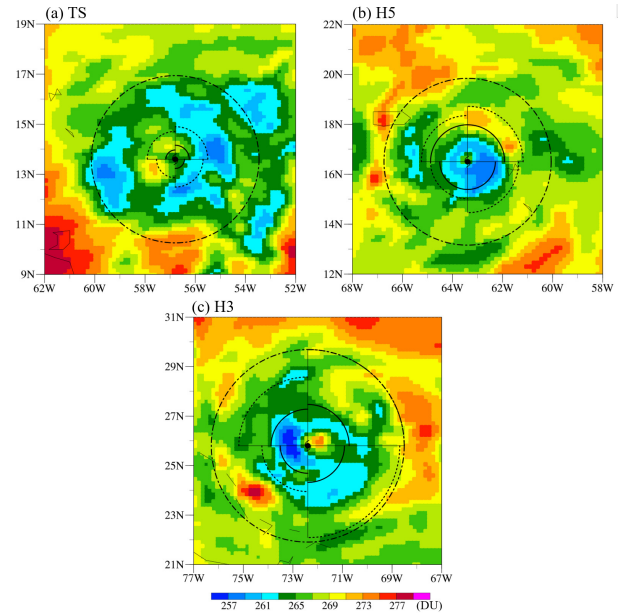


Fig. 3. Spatial distributions of S-NPP OMPS TCO observations (unit: DU) within Hurricane Maria at ~1700 UTC on (a) September 17, (b) September 19, and (c) September 23, 2017. Also indicated are the hurricane center (black hurricane symbol), the radii of the outmost closed isobar (black dash-dotted curve), 34-kt (black dotted curve), and 50-kt (black solid curve) from the best track data.

provide qualitative support to an association of TCO structures to convection within hurricanes. Hurricane top structures are illustrated in Fig. 4 for Hurricane Maria at ~1700 UTC on September 19, 23, and 24, 2017. We note that strong convective areas are generally characterized by low TCO values, representing strong upward lifting of the atmosphere. At the hurricane center, there is a local TCO maximum which is not seen in OMPS low-resolution mode data (figures omitted). The local maximum values of TCO at the center of Hurricane Maria indicate an intrusion of ozone-rich stratospheric air into the core of the hurricane, resulting from subsidence of the stratospheric atmosphere there. This substantiates the conceptual TC model proposed in Rodgers *et al.* [18]. It is also noted that the strong convective areas spread out in a larger domain than the outmost closed isobar when Hurricane Maria reached tropical storm intensity [Fig. 3(a)] and are confined within the outmost closed isobar when Hurricane Maria reached hurricane intensity [Fig. 3(b) and (c)]. The radii of 34- and 50-kt of Maria are larger at hurricane intensities than tropical storm intensities.

IV. METHODOLOGY FOR CHARACTERIZING TC RADIAL STRUCTURES OF OMPS TCO DATA

In order to characterize the TCO intensity and radial variations quantitatively, we define a radius parameter R_{TCO} . There are two steps involved in determining R_{TCO} . First, we apply the six-order even polynomial fitting of the TCO observations versus the radial distance of the hurricane center ($TCO(r) = a_0 + a_1r^2 + a_2r^4 + a_3r^6$) from the TCO observations within 600-km radial distance from the hurricane center. The six-order even polynomial fitting is chosen because it represents well the averaged radial variation of TCO

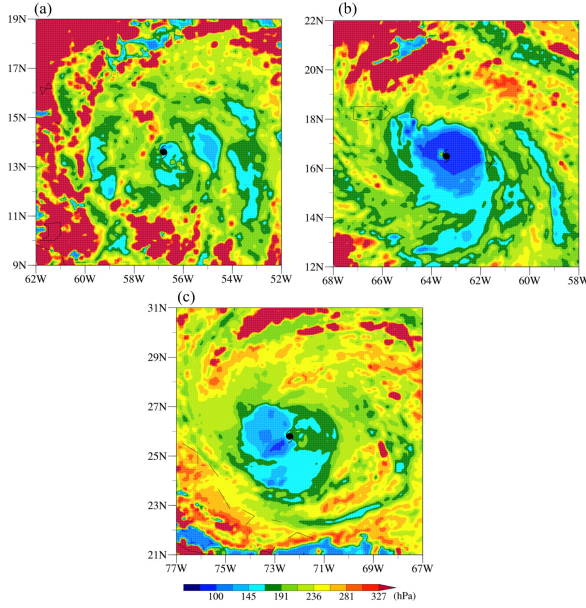


Fig. 4. Spatial distributions of cloud top pressures (unit: hPa) from VIIRS retrieval products within Hurricane Maria at ~ 1700 UTC on (a) September 17, (b) September 19, and (c) September 23, 2017. The best-track-observed hurricane center location is indicated by the black hurricane symbol.

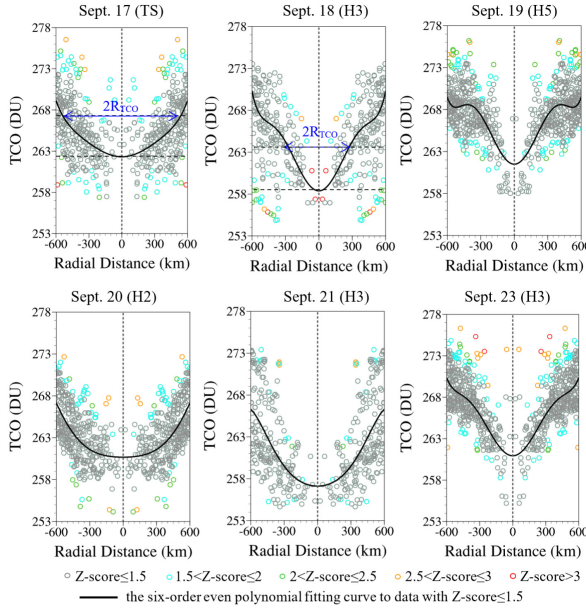


Fig. 5. Scatterplots of OMPS TCO observations versus the radial distance with $Z\text{-score} \leq 1.5$ (gray circle), between 1.5 and 2 (cyan circle), between 2 and 2.5 (green circle), between 2.5 and 3 (orange circle), and > 3 (red circle) within the 600-km radial distances from the best track center location of Hurricane Maria at ~ 1700 UTC from September 17–21 and 23, 2017. Also shown is the six-order even polynomial fitting curve (black) to data with $Z\text{-score} \leq 1.5$.

(see Fig. 5). Then, based on the six-order even polynomial fitting, R_{TCO} is defined as the radial distance where $\text{TCO}(r)$ is higher than the hurricane center by 5 DU (an empirical value), i.e.,

$$\text{TCO}(R_{\text{TCO}}) - \text{TCO}_{\min} = 5\text{DU} \text{ for } R_{\text{eye}} < r \leq R_{\text{TCO}}. \quad (1)$$

When deriving the six-order even polynomial fitting, we use the biweight check [19] to identify and remove outliers.

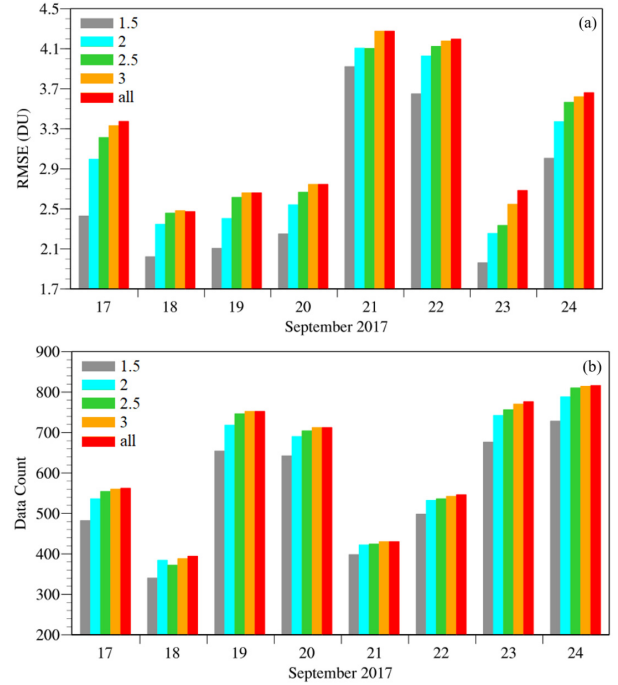


Fig. 6. (a) RMSE of the six-order even polynomial fitting to data within the 600-km radial distances from the best track center location of Hurricane Maria at ~ 1700 UTC from September 17–24, 2017, using data with $Z\text{-score} \leq 1.5, 2, 2.5, 3$, and all data. The data counts are shown in (b).

Because the traditional mean and standard deviation are sometimes greatly distorted by the existence of few extreme outliers, the biweight check employed the median (M) and median absolute deviation (MAD), defined a weighting function (w_i) for each element (x_i) as: $w_i = (x_i - M)/7.5 \times \text{MAD}$ [20], and calculated the biweight mean (\bar{x}_{ib}) and biweight standard deviation (BSD) as

$$\bar{x}_{ib} = M + \frac{\sum_{i=1}^n (x_i - M)(1 - w_i^2)^2}{\sum_{i=1}^n (1 - w_i^2)^2} \quad (2)$$

and

$$\text{BSD} = \frac{\sqrt{n \sum_{i=1}^n (x_i - M)^2 (1 - w_i^2)^4}}{|\sum_{i=1}^n (1 - w_i^2)(1 - 5w_i^2)|}. \quad (3)$$

A $Z\text{-score}$ ($z_i = (x_i - \bar{x}_{ib})/\text{BSD}$) is used as the threshold to identify outliers. For example, $z_i = 1.5$ suggests that x_i is identified as an outlier if it deviates from the biweight means greater than 1.5 times the BSD.

We tested $z_i = 1.5, 2, 2.5$, and 3 to make the final choice of the $Z\text{-score}$ threshold. Fig. 5 shows the scatter plot of the TCO observations versus the radial distance of Hurricane Maria, and indicates the data satisfy $z_i \leq 1.5$ (gray circle), $1.5 \leq z_i \leq 2$ (cyan circle), $2 \leq z_i \leq 2.5$ (green circle), $2.5 \leq z_i \leq 3$ (orange circle), and > 3 (red circle) within the 600-km radial distances from the best track center location of Hurricane Maria.

The six-order even polynomial fittings using the data that satisfying $z_i \leq 1.5, 2, 2.5$, and 3 are derived. The root-mean-square-error (RMSE) and the number of data that were used for this six-order even polynomial fitting are shown in Fig. 6(a) and (b). The threshold of $z_i \leq 1.5$ is chosen in this study because it can greatly decrease the RMSE while

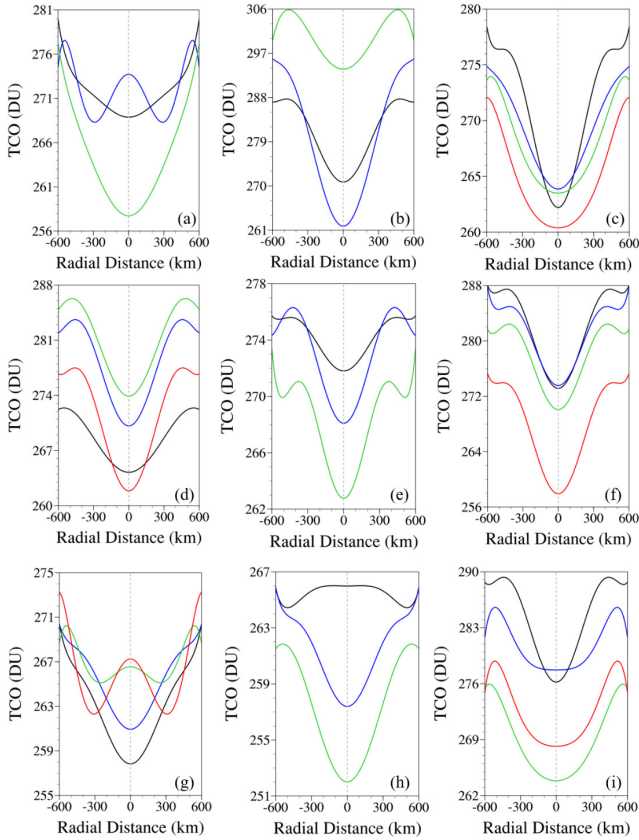


Fig. 7. Six-order even polynomial fitting curve for Hurricane (a) Franklin, (b) Gert, (c) Irma, (d) Jose, (e) Katia, (f) Lee, (g) Maria, (h) Nate, and (i) Ophelia during the time period of four days including the day of the lowest SLP of each hurricane ($t_{\text{lowest SLP}}^{\text{hurricane name}}$). The date period of each hurricane is August 7–9 for Franklin; August 15–17 for Gert; September 3–6 for Irma; September 7–10 for Jose; September 6–8 for Katia; September 25–28 for Lee; September 17–20 for Maria; October 5–7 for Nate; and October 12–15 for Ophelia.

keeping at least 90% of the original data. The six-order even polynomial fitting using data satisfying $z_i \leq 1.5$ is indicated by the black curves in Fig. 5. Following (1), R_{TCO} can be found at the radial distance where it satisfies $\text{TCO}_{\text{min}} + 5 \text{ DU}$. Moreover, the regression models developed in this study could be used as a simple observation operator for OMPS TCO data assimilation in numerical weather prediction models if ozone is not an analysis variable.

V. ASSOCIATIONS OF HURRICANE INTENSITY CHANGES TO TCO STRUCTURAL CHANGES WITHIN HURRICANES

One important application of OMPS TCO observations is to improve the vortex initialization by supplying observed radial structures of hurricane tops. Traditionally, synthetic vortices, i.e., so-called bogus vortices, with either SLP or the surface wind field specified based on a few parameters (e.g., the radius of maximum wind, the position, and the maximum surface wind) are implanted into model initial states [21]–[24]. Construction of other model fields involves the use of geostrophic and hydrostatic equations, the nonlinear balance equation, and empirical vertical structure functions.

In order to analyze the relationship of the changes between TCO radial structure and hurricane intensity, we focus on the period of four days including the day of the lowest SLP of

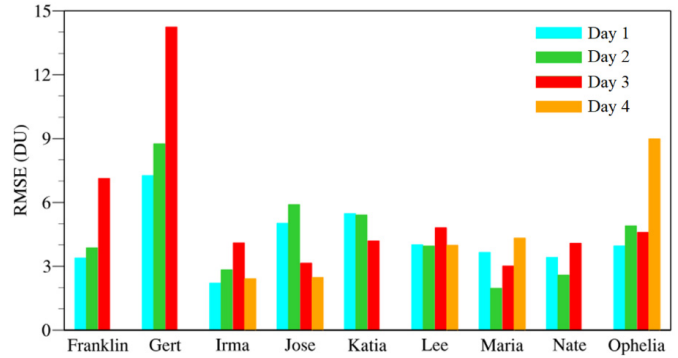


Fig. 8. RMSE of the six-order even polynomial fitting to data within the 600-km radial distances from the best track center location of Hurricane Franklin, Gert, Irma, Jose, Katia, Lee, Maria, Nate, and Ophelia during the time period of four days including the day of the lowest SLP of each hurricane ($t_{\text{lowest SLP}}^{\text{hurricane name}}$). The date period of each hurricane is August 7–9 for Franklin; August 15–17 for Gert; September 3–6 for Irma; September 7–10 for Jose; September 6–8 for Katia; September 25–28 for Lee; September 17–20 for Maria; October 5–7 for Nate; and October 12–15 for Ophelia.

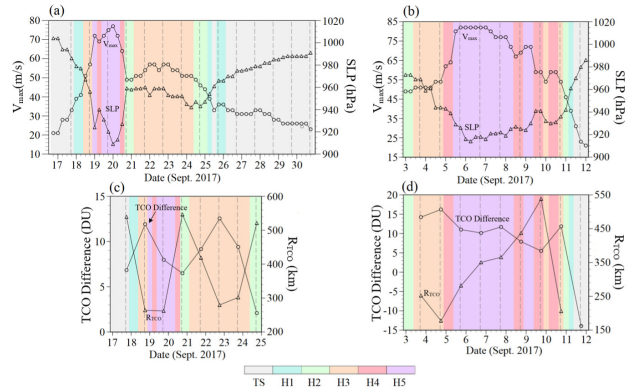


Fig. 9. Temporal evolutions of (a) and (b) the maximum sustained winds (circles, left ordinate) and minimum SLP (triangles, right ordinate), and (c) and (d) the TCO difference ($\text{TCO}_{600\text{km}} - \text{TCO}_0$) (open circles, left ordinate) and the radius R_{TCO} (open triangles, right ordinate) of Hurricane Maria (a) and (c) from 0000 UTC September 17 to 1800 UTC September 30, 2017, and Hurricane Irma (b) and (d) from 1800 UTC September 3 to 0600 UTC September 12 (b) and (d) at 6-h intervals. Also indicated are the S-NPP OMPS observing time at ~1700 UTC each day (vertical dashed line) in (a)–(d). R_{TCO} in (c), and in (d) is the radial distance of the six-order even polynomial fitting curve when its value is 5-DU higher than its minimum value for Hurricane Maria from 1800 UTC September 17 to 1800 UTC September 24, 2017, and for Hurricane Irma from 1800 UTC September 3 to 1800 UTC September 11, respectively.

each hurricane. Having carried out a quality control using the method described in Section IV, the six-order even polynomial fittings within 600-km radial distance for the nine selected ATL hurricanes in 2017 are examined (Fig. 7). The sequence of days is indicated by the order of black, blue, green, and red. Generally, TCO structures vary as the hurricane intensifies. We note that TCOs are generally low within about 500-km radial distances from the hurricane eye where strong convection pushes the tropopause upward. There are also days when a local maximum of TCO near the hurricane center is embedded in the TCO low [Fig. 7(a) and (g)]. The latter is similar to what was pointed out by Zou and Wu [8] using TOMS raw TCO data. Fig. 8 presents the corresponding RMSE. Generally, the RMSE is less than 6 DU.

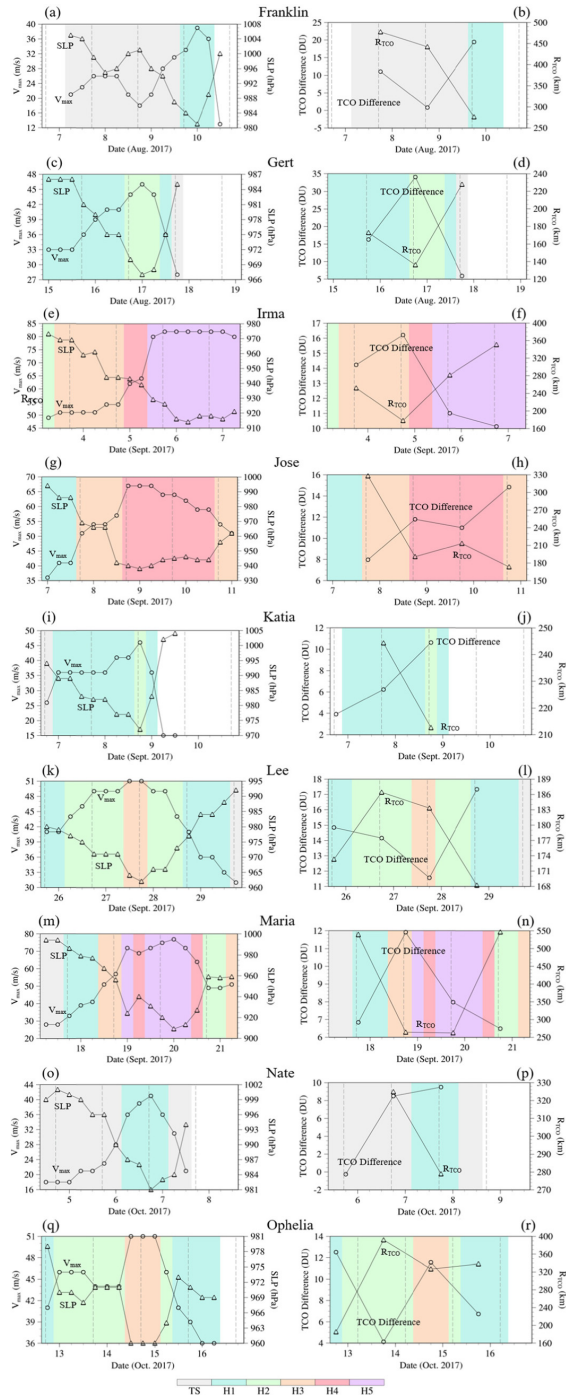


Fig. 10. Temporal evolutions of the maximum sustained winds (circles, left ordinate) and minimum SLP (triangles, right ordinate) (left panels), as well as the TCO difference ($\Delta\text{TCO}_{600\text{km}} = \text{TCO}_{600\text{km}} - \text{TCO}_0$) (open circles, left ordinate) and the radius R_{TCO} (open triangles, right ordinate) (right panels) for Hurricanes (a) and (b) Franklin, (c) and (d) Gert, (e) and (f) Irma, (g) and (h) Jose, (i) and (j) Katia, (k) and (l) Lee, (m) and (n) Maria, (o) and (p) Nate, and (q) and (r) Ophelia during the time period of four days including the day of the lowest SLP of each hurricane ($t_{\text{hurricane name}}^{\text{lowest SLP}}$). The exact time and date of the lowest SLP ($t_{\text{hurricane name}}^{\text{lowest SLP}}$) of each hurricane are 0000 UTC August 10 for Franklin; 0000 UTC August 17 for Gert; 0600 UTC September 6 for Irma; 0000 UTC September 9 for Jose; 1800 UTC September 8 for Katia; 1800 UTC September 27 for Lee; 0000 UTC September 20 for Maria; 1800 UTC October 6 for Nate; and 1200 UTC October 14 for Ophelia.

In order to find out the linkages between the TCO structures and hurricane intensities before they reach the maximum intensity, we can also examine the relationship between R_{TCO}

and the TCO difference ($\Delta\text{TCO}_{600\text{km}} = \text{TCO}_{600\text{km}} - \text{TCO}_0$). Fig. 9(a) and (c) shows the temporal evolution of the hurricane's maximum sustained winds, minimum SLP, TCO difference, and R_{TCO} for Hurricane Maria. Hurricane Maria first reached category 5 at 0000 UTC on September 19. R_{TCO} dropped greatly on September 18, while the TCO difference increased on the same day. As Maria further intensified to its highest strength at 0000 UTC on September 20, R_{TCO} continued to decrease slightly on September 19. The day-to-day variation of Hurricane Irma shows similar characteristics [Fig. 9(b) and (d)]. Irma first reached category 5 at 1200 UTC on September 5. R_{TCO} dropped to its minimum value on September 4 as the TCO difference increased to its maximum value on the same day.

The day-to-day variations of R_{TCO} and TCO difference ($\Delta\text{TCO}_{600\text{km}}$) for the period of four days before and after the selected nine ATL Hurricanes reached their maximum strength were examined (Fig. 10). For Hurricanes Franklin, Gert, Jose, Katia, Lee, and Nate, there is a large drop of R_{TCO} and an accompanying increase of TCO difference ($\Delta\text{TCO}_{600\text{km}}$) one day before reaching their maximum strength. Hurricane Ophelia entered category 3 at 1200 UTC on October 14, while the R_{TCO} started to drop on October 13. Hurricanes Maria and Irma have been discussed previously. This remarkable finding reveals a close link between TCO structure within hurricane and hurricane intensity change, suggesting the potential value of adding satellite TCO data within TCs to construct characteristic radial profiles of the hurricane top structures in vortex initialization.

VI. CONCLUSION

The accurate prediction of hurricane track and intensity changes remains challenging. Advances in satellite remote sensing have provided many types of observations that can capture different structural features of hurricanes. Developing a satellite-observation-based vortex initialization scheme offers a great opportunity to increase the forecast skill of hurricanes. The PV and Montgomery stream-function anomalies at the 315-K, 320-K, 300-K, and 350-K isentropic surfaces are linked to the TCO in the observation operators.

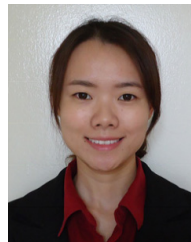
This study uses the S-NPP OMPS TCO data to analyze the associations between the hurricane intensity and TCO structures from nine ATL hurricanes that achieved hurricane intensity in 2017. A six-order even polynomial fitting to TCO data within hurricanes is carried out to obtain the values of two newly defined parameters R_{TCO} and $\Delta\text{TCO}_{600\text{km}}$. The first parameter reveals the size and the second the intensity of the hurricane's structural features in TCO observations within 600-km radial distance from the hurricane center. Results show that TCO distributions are closely related to the structural and intensity changes of hurricanes. In general, a decrease of R_{TCO} and a simultaneous increase of TCO difference $\Delta\text{TCO}_{600\text{km}}$ within a hurricane occur one day before the hurricane reaches its maximum strength. Such a finding suggests that combining the satellite TCO observations with surface and near-surface information in vortex initialization can help produce more realistic initial conditions for hurricane forecasts, leading to more accurate hurricane forecasts.

Some hurricanes are slant, for which the hurricane center at the surface from the best track data may not match well the center in the upper troposphere. Defining the upper troposphere hurricane center using TCO data becomes an active demand, which is planned for future work. A method similar to that recently developed and tested by Hu and Zou [25] will be applied to TCO data for determining hurricane center in the upper troposphere. Results associated with the radial average of TCO data will be reevaluated.

In the future, more hurricane cases (including those that occurred in the Pacific basin) will be analyzed, and a numerical model will be formulated to represent the TCO structure to be incorporated in the vortex initialization scheme for improving the hurricane forecast.

REFERENCES

- [1] G. M. B. Dobson, D. N. Harrison, and J. Lawrence, "Measurements of the amount of ozone in the Earth's atmosphere and its relation to other geophysical condition, Part III," *Proc. Royal Soc. London. Ser. A, Containing Papers Math. Phys. Character*, vol. 122, pp. 456–486, Feb. 1929.
- [2] G. Ohring and H. S. Muench, "Relationship between ozone and meteorological parameters in the lower stratosphere," *J. Meteorol.*, vol. 17, no. 2, pp. 195–206, Apr. 1960.
- [3] L. P. Riishøjgaard and E. Källén, "On the correlation between ozone and potential vorticity for large-scale rossby waves," *J. Geophys. Res., Atmos.*, vol. 102, no. D7, pp. 8793–8804, Apr. 1997.
- [4] Y. J. Orsolini, G. L. Manney, A. Engel, J. Ovarlez, C. Claud, and L. Coy, "Layering in stratospheric profiles of long-lived trace species: Balloonborne observations and modeling," *J. Geophys. Res., Atmos.*, vol. 103, no. D5, pp. 5815–5825, Mar. 1998.
- [5] C. Davis, S. Low-Nam, M. A. Shapiro, X. Zou, and A. J. Krueger, "Direct retrieval of wind from total ozone mapping spectrometer (TOMS) data: Examples from FASTEX," *Quart. J. Roy. Meteorolog. Soc.*, vol. 125, no. 561, pp. 3375–3391, Oct. 1999.
- [6] K.-I. Jang, X. Zou, M. S. F. V. De Pondeca, M. Shapiro, C. Davis, and A. Krueger, "Incorporating TOMS ozone data into the prediction of the Washington January 2000 winter storm," *J. Appl. Meteor.*, vol. 42, pp. 797–812, Jun. 2003.
- [7] Y. Wu and X. Zou, "Numerical test of a simple approach for using TOMS total ozone data in hurricane environment," *Quart. J. Roy. Meteorolog. Soc.*, vol. 134, no. 635, pp. 1397–1408, Jul. 2008.
- [8] X. Zou and Y.-H. Wu, "On the relationship between TOMS ozone and hurricanes," *J. Geophys. Res. Atmos.*, vol. 110, pp. 6109–6123, Mar. 2005.
- [9] S. Penn, "Ozone and temperature structure in a hurricane," *J. Appl. Meteorol.*, vol. 4, no. 2, pp. 212–216, Apr. 1965.
- [10] X. Wu *et al.*, "Evaluation of the sensor data record from the nadir instruments of the ozone mapping profiler suite (OMPS)," *J. Geophys. Res. Atmos.*, vol. 119, pp. 1–13, May 2014.
- [11] C. Pan, F. Weng, and L. Flynn, "Spectral performance and calibration of the Suomi NPP OMPS nadir profiler sensor," *Earth Space Sci.*, vol. 4, no. 12, pp. 737–745, Dec. 2017.
- [12] J. V. Dave and C. L. Mateer, "A preliminary study on the possibility of estimating total atmospheric ozone from satellite measurements," *J. Atmos. Sci.*, vol. 24, no. 4, pp. 414–427, Jul. 1967.
- [13] C. L. Mateer, D. F. Heath, and A. J. Krueger, "Estimation of total ozone from satellite measurements of backscattered ultraviolet Earth radiance," *J. Atmos. Sci.*, vol. 28, no. 7, pp. 1307–1311, Oct. 1971.
- [14] L. Flynn *et al.* (Mar. 2016). *Algorithm Theoretical Basis Document for NOAA NDE OMPS Version 8 Total Column Ozone (V8TOz) Environmental Data Record (EDR) Version 1.0, Satellite Products and Services Review Board*. [Online]. Available: https://www.star.nesdis.noaa.gov/jps/documents/ATBD/ATBD_OMPS_TC_V8TOz_v1.1.pdf
- [15] L. Flynn *et al.*, "Performance of the ozone mapping and profiler suite (OMPS) products," *J. Geophys. Res., Atmos.*, vol. 119, no. 10, pp. 6181–6195, May 2014.
- [16] C. W. Landsea and J. L. Franklin, "Atlantic hurricane database uncertainty and presentation of a new database format," *Monthly Weather Rev.*, vol. 141, no. 10, pp. 3576–3592, Oct. 2013.
- [17] E. B. Rodgers, S. W. Chang, J. Stout, J. Steranka, and J.-J. Shi, "Satellite observations of variations in tropical cyclone convection caused by upper-tropospheric troughs," *J. Appl. Meteorol.*, vol. 30, no. 8, pp. 1163–1184, Aug. 1991.
- [18] E. B. Rodgers, J. Stout, J. Steranka, and S. Chang, "Tropical cyclone-upper atmospheric interaction as inferred from satellite total ozone observations," *J. Appl. Meteorol.*, vol. 29, no. 9, pp. 934–954, Sep. 1990.
- [19] X. Zou and Z. Zeng, "A quality control procedure for GPS radio occultation data," *J. Geophys. Res.*, vol. 111, no. D2, pp. 1–13, 2006.
- [20] J. R. Lanzante, "Resistant, robust and nonparametric techniques for the analysis of climate data: Theory and examples, including applications to historical radiosonde station data," *Int. J. Climatol.*, vol. 16, no. 11, pp. 1197–1226, Nov. 1996.
- [21] Y. Kurihara, M. A. Bender, R. E. Tuleya, and R. J. Ross, "Prediction experiments of Hurricane Gloria (1985) using a multiply nested movable mesh model," *Monthly Weather Rev.*, vol. 118, no. 10, pp. 2185–2198, Oct. 1990.
- [22] S. J. Lord, "A bogusing system for vortex circulations in the national meteorological center global forecast model," in *Proc. 19th Conf. Hurricanes Tropical Meteorol.*, Miami, FL, USA: American Meteorological Society, 1991, pp. 328–330.
- [23] T. V. Thu and T. N. Krishnamurti, "Vortex initialization for typhoon track prediction," *Meteorol. Atmos. Phys.*, vol. 47, nos. 2–4, pp. 117–126, 1992.
- [24] X. Zou and Q. Xiao, "Studies on the initialization and simulation of a mature hurricane using a variational bogus data assimilation scheme," *J. Atmos. Sci.*, vol. 57, no. 6, pp. 836–860, Mar. 2000.
- [25] Y. Hu and X. Zou, "Comparison of tropical cyclone center positions determined from satellite observations at infrared and microwave frequencies," *J. Atmos. Ocean. Technol.*, vol. 37, no. 11, pp. 2101–2115, Nov. 2020.



Lin Lin received the B.Sc. degree from the Nanjing University of Information Science and Technology (NUIST), Nanjing, China, in 2002, and the master's and Ph.D. degrees in meteorology from the Florida State University (FSU), Tallahassee, FL, USA, in 2005 and 2009, respectively.

She is with the Earth System Science Interdisciplinary Center (ESSIC), University of Maryland, College Park, MD, USA. Her primary interests are calibration of satellite data at microwave wavelengths; intercalibration of satellite data using global positioning system (GPS) radio occultation (RO) data; simulations of the microwave instrument using the community radiative transfer model (CRTM), the monochromatic radiative transfer model (MonoRTM), and line-by-line radiative transfer model (LBLRTM); development of quality control techniques for improving uses of satellite data in numerical weather prediction models; direct assimilation of microwave radiances in the hurricane weather research and forecasting (HWRF) system; impact of direct assimilation of microwave radiances on hurricane forecasts; cloudy radiances through advanced radiative transfer models; cloud detection using the double- CO_2 band in the cross-track infrared sounder (CrIS); and exploring the relationship between climate change and human science.



Xiaolei Zou (Member, IEEE) received the Ph.D. degree from the Institute of Atmospheric Physics, Academia Sinica, Beijing, China, in 1988.

She developed the National Meteorological Center (now the National Center for Environmental Prediction) medium-range global forecast model 4-D-Var system with full physics during 1989–1993, and the fifth generation Penn State/NCAR Mesoscale Model (MM5) 4-D-Var system during 1993–1997. She has worked on GPS radio occultation data assimilation since 1993. From 1997 to 2014, she was a Professor with the Department of Earth, Ocean, and Atmospheric Science, Florida State University, Tallahassee, FL, USA. During 2014–2018, she has been working mainly on satellite data assimilation for quantitative precipitation forecasts and hurricane track and intensity forecasts at the Earth System Science Interdisciplinary Center (ESSIC), University of Maryland. She has authored over 165 articles in peer-reviewed journals.

Dr. Zou was the recipient of the 2008 American Meteorological Society Fellow Award for her outstanding contributions to the applications of satellite data in the numerical-weather-prediction models and the education in data assimilation.